

Accepted Manuscript

Structure-based drug design, synthesis, *In vitro*, and *In vivo* biological evaluation of indole-based biomimetic analogs targeting estrogen receptor- α inhibition

Moataz S. Hendy, Aya A. Ali, Lubna Ahmed, Reham Hossam, Alaa Mostafa, Mohamed M. Elmazar, Bassem H. Naguib, Yasmeen M. Attia, Mahmoud Salama Ahmed

PII: S0223-5234(19)30088-1

DOI: <https://doi.org/10.1016/j.ejmech.2019.01.068>

Reference: EJMECH 11075

To appear in: *European Journal of Medicinal Chemistry*

Received Date: 16 November 2018

Revised Date: 14 January 2019

Accepted Date: 28 January 2019

Please cite this article as: M.S. Hendy, A.A. Ali, L. Ahmed, R. Hossam, A. Mostafa, M.M. Elmazar, B.H. Naguib, Y.M. Attia, M.S. Ahmed, Structure-based drug design, synthesis, *In vitro*, and *In vivo* biological evaluation of indole-based biomimetic analogs targeting estrogen receptor- α inhibition, *European Journal of Medicinal Chemistry* (2019), doi: <https://doi.org/10.1016/j.ejmech.2019.01.068>.

This is a PDF file of an unedited manuscript that has been accepted for publication. As a service to our customers we are providing this early version of the manuscript. The manuscript will undergo copyediting, typesetting, and review of the resulting proof before it is published in its final form. Please note that during the production process errors may be discovered which could affect the content, and all legal disclaimers that apply to the journal pertain.



Structure-Based Drug Design, Synthesis, *In vitro*, and *In vivo* Biological Evaluation of Indole-Based Biomimetic Analogs Targeting Estrogen Receptor- α Inhibition

Moataz S. Hendy^{1, 2}, Aya A. Ali^{2, 3}, Lubna Ahmed⁴, Reham Hossam⁴, Alaa Mostafa⁴, Mohamed M. Elmazar^{2, 3}, Bassem H. Naguib^{1, 2, 5}, Yasmeen M. Attia^{2, 3*}, Mahmoud Salama Ahmed^{1, 2, 6*}

¹Department of Pharmaceutical Chemistry, Faculty of Pharmacy, The British University in Egypt, El-Sherouk, Cairo, Egypt

²Center of Drug Research and Development (CDRD), The British University in Egypt, El-Sherouk, Cairo, Egypt

³Department of Pharmacology, Faculty of Pharmacy, The British University in Egypt, El-Sherouk, Cairo, Egypt

⁴Faculty of Pharmacy, The British University in Egypt, El-Sherouk, Cairo, Egypt

⁵Department of Pharmaceutical Organic Chemistry, Faculty of Pharmacy, Cairo University, Cairo, Egypt

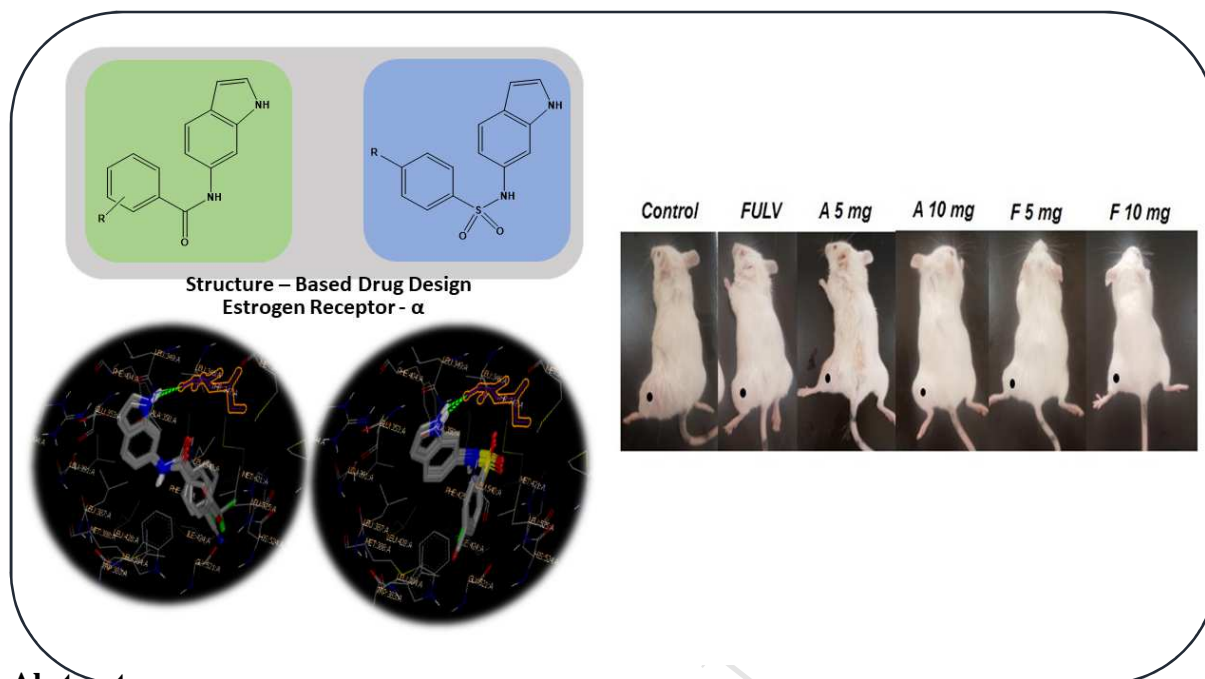
⁶Department of Internal Medicine, Division of Cardiology, University of Texas Southwestern Medical Center, Dallas, Texas, USA

*Corresponding Authors: Mahmoud Salama Ahmed; Email Address: Mahmoud.salama@bue.edu.eg, Yasmeen M. Attia; Email Address: Yasmeen.attia@bue.edu.eg

Highlights:

- Indole-based analogs mimicking steroids scaffold were designed and synthesized.
- All newly synthesized analogs enrolled into *in vitro* screening against estrogen receptor dependent cancer cell lines and estrogen receptor binding assays.
- YMA-005 and YMA-006 showed significant reduction in the tumor size in the animal model of Ehrlich ascites carcinoma solid tumor at two dose levels.
- YMA-005 and YMA-006 showed reductions in the immune-histochemical expression of ER- α expression at two different dose levels.

Graphical Abstract:

**Abstract:**

Offering novel scaffolds targeting estrogen receptor creates huge necessity to overcome the evolving resistance developed by tumors. Structure-based drug design coupled with ring opening strategy of the steroids skeleton revealed the potential of indole-based analogs to be synthesized targeting the ligand binding domain of estrogen receptor- α . *In vitro* studies revealed the potential of the total sub-classes of the synthesized analogs to show anti-proliferative activity against estrogen receptor-dependent cancer cell lines at IC_{50} ranging from 28.23 to 57.13 μ M. This was further validated by evaluating the potential of the synthesized analogs to compete along with estradiol *via* ER- α ELISA assay to show inhibitory profile at IC_{50} ranging from 1.76 to 204.75 nM. Two analogs (YMA-005 and YMA-006) showed significant reduction in tumor size at two dose levels with extensive degeneration and necrosis. Both YMA-005 and YMA-006 showed *in-situ* reduction of ER- α Immunohistochemical expression at both dose levels. Ultimately, novel analogs of indole-based biomimetic of estrone scaffolds were offered as estrogen receptor- α inhibitors.

Keywords:

Indole, Biologically Inspired Organic Synthesis, Estrogen Receptor- α , Breast Cancer

1. Introduction:

Human Breast carcinoma is the second leading cause for mortality among women. According to the latest statistics issued by American Cancer Society in 2017, reporting an estimate of 252,710 newly diagnosed cases of invasive breast cancer, 63,410 newly diagnosed cases of breast carcinoma *in situ*, and 40,610 breast cancer deaths [1]. Breast cancer has been classified into four main categories; where estrogen receptor- α (ER- α positive) sub-type is the principle cause for 60-80% of breast cancer cases [2,3]. ER is a nuclear receptor with known physiological functions regulating normal growth, development of reproductive organs, protecting the cardiovascular system by decreasing cholesterol level, and bone homeostasis [4]. The structural organization of ER is composed of two main domains, DNA binding domain (DBD) and ligand-binding domain (LBD) linked by hinge region, in addition to N and C terminal domains [5].

ER is expressed in two isoforms, ER- α and ER- β , where they share up to 95% homology at the DBD and 55% homology at the LBD [5]. Typically, 17 β -estradiol is acting as agonist for induction favorable conformation for coactivator binding surface of the LBD called activation function-2 (AF2), where helix-12 (H-12) harbors across helix-11 and helix-3 (H-11 and H-3) leading to formation of one side of the AF2 surface, leading to promotion of ER- α gene expression [6]. Estrogen and estradiol have been known for their promoter role for cancer proliferation accompanied with increased tumor invasion. Therefore, the conceptual basics for tackling ER dependent breast cancer are built on development of new chemical entities inhibiting the binding of estrone family to ER.

Several FDA approved drugs, such as Tamoxifen led to revolutionary step towards treatment of ER dependent breast cancer, acting as agonist at low doses and antagonist at high doses to be categorized as selective estrogen receptor modulator (SERM) [7]. In addition, Fulvestrant showed potent anti-estrogenic activity in all tissues with no agonistic activity to be known as selective estrogen receptor down regulator (SERD) [8]. Both of SERM and SERD showed their antagonism *via* competing with the natural endogenous substrates at LBD to inhibit ER- α gene expression [8]. However, the endocrine therapy/chemotherapeutic agents are typically associated with the evolution of drug resistance; in other words, cancer cells develop resistance against the administered drugs; leading to serious complications [9]. Different scaffolds were synthesized to target estrogen receptor whether inspired from Estrone or Tamoxifen skeleton lacking the typical bulky side chain [10-12], as shown in **Figure 1**.

Herein, two fundamental strategies in the drug discovery, biologically inspired organic synthesis (BIOS) and ring opening based on the steroidal skeleton at B/C ring juncture were explored to assemble novel indole-based scaffolds that can be categorized as conformers to biomimic estradiol configuration targeting ER- α , as shown in **Figure 2**. The whole design strategy focused on overcoming the rigidity present at the steroidal scaffold to offer structural flexibility *via* assembly of indole ring along with substituted either sulfonamide or carboxamide derivatives. This was followed by *in vitro* biological screening against ER-dependent breast cancer cell lines, inhibitory profiles for the synthesized analogs against ER- α . This was followed by selecting two top hits *in vivo* biological evaluation.

2. Results and Discussion:

2.1. *In silico* virtual screening:

The initial hypothesis started with employment of structure-based drug design (SBDD) strategy *via* design of a virtual library of energy-minimized analogs including amide and sulfonamide analogs coupled with 6-amino indole. The library underwent multi-conformer generation for molecular docking study against ER- α receptor (PDB ID: 1ERE), to be sorted out based on the binding energy profiles related to the endogenous substrates of the receptors of interest [13].

The indole-based analogs exhibited promising binding affinity towards ligand binding domain (LBD) of ER- α *via* hydrophobic–hydrophobic interactions and interesting hydrogen bond between –NH of indole ring along with Threonine (Thr) 347: A, as shown in **Figure 3**. Thr 347: A is one of the featured amino acid residues for structural antagonism towards ER- α [14,15], suggesting that the analogs will disrupt H-12 interaction, dislocating the co-activators, leading to inhibition of gene expression.

2.2. Synthetic strategy and chemistry:

The structural insights of inhibitors design showed the significance of employment of BIOS strategy coupled with ring opening to end up with conformational mimetics to steroid scaffolds while overcoming the known steroidal adverse effects. Synthetic schemes towards synthesis of the best scoring indole-based ligands, therefore, were outlined.

2.2.1. General synthetic pathway for indole-based analogs:

Ten final indole-based analogs were selected from the library and synthesized for initial biological screening. Initially, reduction of 6-nitro indole to 6-amino indole was accomplished using stannous chloride conditions [16]. Acylation and sulfonylation of 6-amino indole with substituted benzoyl chlorides and substituted benzene sulfonyl chlorides in basic conditions and aprotic solvents under nitrogen ended up with two main classes of substituted N-(*1H*-indol-6-yl)

benzamide and substituted N-(*1H*-indol-6-yl) benzene sulfonamide, respectively, as shown in **schemes 1 and 2**.

Coupling of substituted benzoyl chlorides with substituted 4- or 5-amino indole derivatives or coupling of substituted benzene sulfonyl chlorides with substituted 4-amino indole derivatives were previously reported [17-20]. The present methodology for the synthesis of substituted N-(*1H*-indol-6-yl) benzamide and substituted N-(*1H*-indol-6-yl) benzene sulfonamide in basic conditions targeting estrogen receptor, however, is newly reported. Wherein, the whole objective of the synthesis is to offer novel non-steroidal scaffold based on the initial SBDD screening to create focused library.

2.3. Biological Screening:

2.3.1. *In vitro* anti-proliferative MTT assay against estrogen receptor dependent cancer cell lines: The synthesized indole-based analogs underwent cell viability assays against estrogen receptor dependent cancer cell lines (MCF-7 and T47D cell lines) to exhibit inhibitory behavior ranging from 28.23 to 57.13 μM , compared to Tamoxifen (34 μM), as shown in **table 1**. This suggested the potential of the synthesized analogs to have inhibitory activities against proliferation of breast cancer cell lines.

2.3.2. ER- α competitive binding assay:

The synthesized analogs underwent ER- α ELISA competitive binding assays to evaluate the potential of the analogs to compete along with estrogen on LBD, where they showed the inhibitory competitive manner against ER- α ranging from 1.76 to 204.75 nM, as shown in **table 1**. Two representative compounds from each class, YMA-005 and YMA-006, were further selected for investigation of their *in vivo* biological behavior.

2.3.3. *In vivo* anticancer activity and safety of YMA-005 and YMA-006:

Two compounds, YMA-005 and YMA-006, were selected for further *in vivo* animal studies based on their promising *in vitro* activity. The safety of the selected compounds was observed in normal mice at a dose of 10 mg/mouse where they were observed for short-term acute signs of toxicity. No toxic signs were observed and the animals showed no signs of behavioral changes. Moreover, no mortality was seen in all groups treated with either YMA-005 or YMA-006. The two compounds were tested at two dose levels, 5 and 10 mg/mouse, in an animal model of Ehrlich ascites carcinoma (EAC) solid tumor and their efficacy was compared to that of Fulvestrant (FULV). Both compounds, especially YMA-005, showed better reductions in tumor size, compared to both control and FULV-treated groups. After nine and twelve days of treatment, YMA-005 caused significant reductions in tumor size at both low and high doses, compared to FULV. On day fifteen after treatment and just before scarification, low dose of YMA-005 and high dose of YMA-006 showed reductions in tumor volume, compared to FULV, whereas the remaining compounds showed only significant reductions compared to untreated control group. In addition, there was no significant change in body weights among different treated groups compared to control group, as shown in **Figure 4**.

2.3.4. Histopathological examination and necrotic indices:

The effect of YMA-005 and YMA-006 treatments on the histopathological changes in the present model was examined using hematoxylin and eosin (H&E) staining for necrotic changes / areas of malignant viable cells. The group treated with a low dose of YMA-006 showed tumor sections with the least areas of necrosis. However, YMA-006 (10 mg)-treated group showed mixed viable and focal necrotic areas in the deeper parts of the tumor mass. YMA-005 (10 mg)-treated group, on the other hand, demonstrated extensive necrotic areas as well as degenerated tumor cells and less extensive areas of viable tumor cells in the outer zone of the tumor mass, as

shown in **Figures 5 and 6**. The necrotic indices in H&E-stained tumor sections belonging to the different groups were also estimated where low dose of YMA-005 showed the highest index compared to both control and FULV-treated groups.

2.3.5. Estrogen- α expression:

Primary monoclonal antibody against ER- α receptor was used to evaluate the effect of compounds on ER- α expression in tumor sections of different groups. Both YMA-005 and YMA-006 at the two dose levels showed reductions in ER- α expression, compared to control and FULV-treated groups. YMA-005 showed 64.71% and 35.30% reduction in ER- α expression, compared to control, and 57.75% and 22.54% reduction, compared to FULV at low and high doses, respectively, as shown in **Figure 7**. Likewise, YMA-006 showed 58.24% and 37.65% reduction, compared to control, as well as 50% and 25.35% reduction, compared to FULV at low and high doses, respectively. Expression of ER- α in EAC animal model was reported to decrease with estrogen receptor modulators.

2.3.6. Structural activity relationship analysis:

Applying BIOS and ring opening strategies enabled us to offer novel pharmacophore as indole-based biomimetic analogs to steroidal scaffolds with inhibitory activity against ER- α dependent breast cancer. We managed to synthesize top ten compounds based on structure-based drug design for indole-based analogs representing two main classes; (1) substituted N-(1*H*-indole-6-yl) benzamide derivatives and (2) substituted N-(1*H*-indol-6-yl) benzene sulfonamide. *In vitro* screening against ER- α dependent breast cancer cell lines and ER- α competitive binding assay were executed to elucidate preliminary structural activity correlation. Generally, benzamide analogs showed better inhibitory profiles against MCF-7 and T-47D cell lines as well as better inhibitory competitive binding affinity towards ER- α .

The substituted N-(1*H*-indole-6-yl) benzamide derivatives showed inhibitory profiles in the following manner 3-trifluoromethyl > 4-cyano > 4-bromo > 4-trifluoromethyl > 4-fluoro. The electron-withdrawing group showed promising binding affinity. Trifluoromethyl at *meta* position showed the best binding affinity with respect to the energy profile prior to the synthesis to show the best biological activity against ER- α dependent breast cancer cell lines and ER- α competitive binding assay.

The substituted N-(1*H*-indol-6-yl) benzene sulfonamide showed inhibitory profiles in the following manner 4-fluoro > 4-methoxy > 4-bromo > 4-chloro > 4-methyl. This suggests that the presence of electron withdrawing group could be important for the activity against ER- α dependent breast cancer cell lines and ER- α competitive binding assay.

This study represents an introduction of novel synthetically feasible scaffolds targeting ER- α dependent breast cancer.

3. Conclusions:

Two sets of indole-based class were designed targeting estrogen receptor based on two main approaches; BIOS starting with steroidal scaffolds with its known biological activity, followed by ring opening strategy. Indole-based analogs were initially screened *via* SBDD principles showing well-tailored binding affinity towards ER *via* hydrophobic-hydrophobic interactions at the LBD and hydrogen bond along with THR 347:A. Ten indole-based derivatives were synthesized *via* two step reactions; starting with reduction of 6-nitroindole, followed by nucleophilic substitution reactions with benzoyl or benzene sulfonyl chlorides in basic conditions. YMA-005 and YMA-006 s inhibit cell proliferation of ER-dependent cancer cell lines, which was further confirmed by ER- α inhibitory assay. *In vivo* studies where they exhibited significant reduction in tumor size of EAC-bearing mice at two dose levels with

remarkable necrosis and reduction in ER- α expression in tumor sections. In the present study, promising novel indole-based scaffolds as biomimetic analogs targeting estrogen receptor were developed.

4. Experimental Section:

4.1. *In silico* virtual screening

A virtual library of indole-based analogs along with estradiol and estrone structures were designed in the two-dimensional (2D) structures. The structures were exported to three-dimensional (3D) configuration to be ready for energy minimized using MMFF94 force field. The energy minimized compounds underwent semi-flexible docking using Omega and FRED along with the box assigned for the receptor (PDB ID: 1ERE), as previously described [21-25].

4.2. Chemistry

4.2.1. General: Spectroscopic data (^1H and ^{13}C NMR spectra) were done using Bruker AVANCE-400 MHz and 100 MHz NMR spectrometer, in deuterated solvents of dimethyl sulfoxide (DMSO-d_6) and chloroform (CDCl_3). Chemical shifts (δ) are reported in ppm and coupling J -constants in Hz. The signals are reported as singlet (s), doublet (d), triplet (t), quartet (q), or multiplet (m). TLC analyses were performed using pre-coated silica gel sheets visualized at short and long wavelengths. Mass spectra were processed at Al-Azhar University, Nasr City, Cairo, Egypt, using Thermo-scientific GCMS ISQ. Chemicals and reagents were purchased from Sigma Aldrich and used as received.

4.2.2. Synthesis of 6-amino indole:

To a solution of 6-nitro indole (1 eq.) in a mixture of acetic acid (0.15 M) and hydrochloric acid (0.6 M), SnCl₂ (10 eq.) was added. The reaction mixture proceeded and ¹H NMR was recorded, as previously reported [16].

4.2.3. General Synthesis of substituted N-(1*H*-indole-6-yl) benzamide derivatives:

A flask was charged with 6-amino Indole (1eq.) in the presence of dichloromethane (DCM, 0.5 M) and E₃N (1.2 eq.) under nitrogen at 0 °C. This was followed by addition of substituted benzoyl chlorides (1 eq.) to stir at room temperature overnight. The reaction mixture was quenched by water to be extracted with ethyl acetate and dried over anhydrous Na₂SO₄. The ethyl acetate layer was evaporated *in vacuo*. The crude product was purified using silica gel column chromatography using ethyl acetate/hexane solvent mixture (50:50) to obtain substituted N-(1*H*-indole-6-yl) benzamide derivatives.

4.2.3.1. YMA-001: 4-fluoro-N-(1*H*-indol-6-yl) benzamide; white powder; yield, 90%; ¹H NMR (400 MHz, DMSO-d₆): δ 11.07 (s, 1H), 10.18 (s, 1H), 8.06 (m, 3H), 7.49 (d, *J*= 8.31 Hz, 1H), 7.27-7.39 (m, 4H), 6.39 (d, *J*= 8.31 Hz, 1H). Addition of D₂O quenched -NH peaks at δ 11.07 and 10.18. ¹³C NMR (100 MHz, DMSO-d₆): 165.5, 164.9, 163.6, 139.6, 131.9, 130.9, 130.8, 129.1, 120.9, 120.4, 115.9, 115.7; MS calcd for C₁₅H₁₁FN₂O, 254.09, found *m/z*: 253.26 [M⁺-1, 100%]

4.2.3.2. YMA-002: N-(1*H*-indol-6-yl)-4-(trifluoromethyl) benzamide, buff white powder; yield, 75%. ¹H NMR (400 MHz, DMSO-d₆): δ 10.50 (s, 1H), 10.08 (s, 1H), 8.35 - 8.22 (m, 1H), 7.65 (d, *J* = 8.07 Hz, 1H), 7.49 (d, *J* = 8.07 Hz, 1H), 6.96 - 6.86 (m, 3H), 6.70 -6.60 (m, 2H), 6.50 (s, 1H). ¹³C (100 MHz, DMSO-d₆): 166.5, 137.6, 135.9, 134.6, 130.8, 129.1, 126.7, 126.6, 124.9, 124.5, 120.4, 113.5, 104.6, 102.1; M.S. calcd for C₁₆ H₁₁F₃N₂O, 304.08; found *m/z*: 303.26 [M⁺-1, 100 %]

4.2.3.3. YMA-003: 4-cyano-N-(*1H*-indol-6-yl) benzamide, white powder; yield, 80%. ¹H NMR (400 MHz, DMSO-*d*₆): δ 11.10 (s, 1H), 10.01 (s, 1H), 8.14 - 8.01 (m, 5H), 7.50 (d, *J* = 8.31 Hz, 1H), 7.30 (d, *J* = 7.82 Hz, 2H), 6.39 (s, 1H). M.S. calcd for C₁₆ H₁₁N₃O, 261.09; found *m/z*: 260.28 [*M*⁺-1, 100%]

4.2.3.4. YMA-004: 4-bromo-N-(*1H*-indol-6-yl) benzamide, yellowish white powder; yield, 75%. ¹H NMR (400 MHz, DMSO-*d*₆): δ 11.50 (s, 1H), 10.20 (s, 1H), 8.06 (m, 3H), 7.49 (d, *J* = 8.31 Hz, 1H), 7.27-7.39 (m, 4H), 6.39 (d, *J* = 8.31 Hz, 1H). ¹³C NMR (100 MHz, DMSO-*d*₆): δ 165.1, 135.6, 132.5, 131.7, 129.8, 125.2, 124.8, 120.2, 115.3, 115.01, 113.2, 102.5, 100.6. M.S. calcd for C₁₅H₁₁BrN₂O, 314.01; found *m/z*: 313.17 [*M*⁺-1, 70%]

4.2.3.5. YMA-005: N-(*1H*-indol-6-yl)-3-(trifluoromethyl) benzamide, buff white powder; yield, 85%. ¹H NMR (400 MHz, DMSO-*d*₆): δ 11.06 (s, 1H), 10.35 (s, 1H), 8.59 – 7.60 (m, 4H), 7.35 (d, *J* = 2.69 Hz, 2H), 7.09 (d, *J* = 2.69 Hz, 2H), 6.65 (s, 1H). ¹³C NMR (100 MHz, DMSO-*d*₆): δ 169.5, 135.3, 132.5, 131.2, 130.0, 129.9, 125.0, 124.8, 119.01, 115.09, 114.8, 112.9, 103.7, 101.5. M.S. calcd for C₁₆ H₁₁F₃N₂O, 304.08; found *m/z*: 303.26 [*M*⁺-1, 100%]

4.2.4. General Synthesis of substituted N-(*1H*-indol-6-yl) benzene sulfonamide derivatives:

A flask was charged with 6-amino indole (1 eq.) in the presence of mixture of anhydrous THF / Ether (1:1, 0.5 M) and anhydrous pyridine (1.2 eq.) under nitrogen at 0 °C. This was followed by addition of substituted benzene sulfonyl chloride (1eq.) to stir at room temperature overnight. The reaction mixture was quenched by addition of water to be extracted with ethyl acetate and dried over anhydrous Na₂SO₄. The ethyl acetate layer was allowed to evaporate *in vacuo*. The crude product was purified using silica gel column chromatography using ethyl acetate / hexane mixture (60:40) to obtain **substituted N-(*1H*-indol-6-yl) benzene sulfonamide**.

4.2.4.1. YMA-006: 4-fluoro-N-(*1H*-indol-6-yl) benzene sulfonamide; purple powder; yield, 95%; ^1H NMR (400 MHz, CDCl_3): δ 8.39 (s, 1H), 7.59 (d, $J = 2.69$ Hz, 2H), 7.30 (d, $J = 2.69$ Hz, 2H), 7.22 (s, 1H), 6.83 – 6.78 (m, 2H), 6.20 (s, 1H). ^{13}C NMR (100 MHz, CDCl_3): δ 166.3, 163.8, 135.8, 134.8, 130.2, 130.1, 130.0, 126.3, 125.5, 121.1, 116.2, 116.2, 116.0, 106.8, 102.2; M.S. calcd for $\text{C}_{14}\text{H}_{11}\text{FN}_2\text{O}_2\text{S}$, 290.05; found m/z : 289.31 [$\text{M}^+ - 1$, 100%]

4.2.4.2. YMA-007: 4-chloro-N-(*1H*-indol-6-yl) benzene sulfonamide; dark tan powder; yield, 85%; ^1H NMR (400 MHz, CDCl_3): δ 8.25 (s, 1H), 7.55 (d, $J = 8.31$ Hz, 2H), 7.36 (d, $J = 8.31$ Hz, 2H), 7.22 (s, 1H), 7.09 (m, 1H), 6.58 (d, $J = 7.82$ Hz, 1H), 6.39 (s, 1H). ^{13}C NMR (100 MHz, CDCl_3): δ 139.3, 137.4, 135.8, 130.1, 129.2, 128.7, 126.4, 125.3, 121.2, 116.3, 106.9, 102.4; M.S. calcd for $\text{C}_{14}\text{H}_{11}\text{ClN}_2\text{O}_2\text{S}$, 306.02; found m/z : 306.00 [M^+ , 100%]

4.2.4.3. YMA-008: 4-Methyl-N-(*1H*-indol-6-yl) benzene sulfonamide; purple powder; yield, 90%; ^1H NMR (400 MHz, CDCl_3): δ 8.21 (s, 1H), 7.53 (d, $J = 7.82$ Hz, 2H), 7.35 (d, $J = 8.07$ Hz, 2H), 7.26 (s, 1H), 7.08 – 7.06 (m, 1H), 6.58 (d, $J = 8.07$, 1H), 6.39 (s, 1H), 2.26 (s, 3H). ^{13}C NMR (100 MHz, CDCl_3): δ 143.6, 136.1, 135.8, 130.7, 129.5, 127.3, 126.1, 125.0, 121.0, 116.1, 106.4, 102.4, 21.5; M.S. calcd for $\text{C}_{15}\text{H}_{14}\text{N}_2\text{O}_2\text{S}$, 286.08; found m/z : 285.35 [$\text{M}^+ - 1$, 100%]

4.2.4.4. YMA-009: 4-Bromo-N-(*1H*-indol-6-yl) benzene sulfonamide; purple powder; yield, 80%; ^1H NMR (400 MHz, CDCl_3): δ 8.29 (s, 1H), 7.47 (d, $J = 8.07$ Hz, 2H), 7.36 (d, $J = 8.07$ Hz, 2H), 7.22 (s, 1H), 7.07 (s, 1H), 6.59 (d, $J = 8.31$, 1H), 6.38 (s, 1H). ^{13}C NMR (100 MHz, CDCl_3): δ 138.0, 135.8, 132.2, 130.0, 129.1, 130.8, 128.8, 127.8, 126.4, 125.3, 121.2, 116.3, 106.9, 102.5; M.S. calcd for $\text{C}_{14}\text{H}_{11}\text{BrN}_2\text{O}_2\text{S}$, 351.97; found m/z : 350.21 [$\text{M}^+ - 2$, 70%]

4.2.4.5. YMA-010: 4-Methoxy-N-(*1H*-indol-6-yl) benzene sulfonamide; purple powder; yield, 90%; ^1H NMR (400 MHz, CDCl_3) δ 8.20 (s, 1H), 7.56 (d, $J = 7.82$ Hz, 2H), 7.38 (d, $J = 8.07$ Hz, 2H), 7.28 (s, 1H), 7.10 – 7.08 (m, 1H), 6.60 (d, $J = 8.07$, 1H), 6.40 (s, 1H), 3.81 (s, 3H). ^{13}C

NMR (100 MHz, CDCl₃); δ 143.6, 136.1, 135.8, 130.7, 129.5, 127.3, 126.1, 125.0, 121.0, 116.1, 106.4, 102.4, 57.5. M.S. calcd for C₁₅H₁₄N₂O₃S, 302.07; found m/z : 301.5 [M⁺-1, 100%]

4.3. Biological Screening:

4.3.1. *In vitro* anti-proliferative MTT assay against MCF-7 and T47D cell lines:

Cell Lines: Cells were obtained from American Type Culture Collection (ATCC). The cell lines (MCF-7 and T47D) were sub-cultured in a similar fashion mode, as previously reported [26], before being treated without or with 5- fold serial dilutions of YMA compounds in triplicates for 24 h. The cells were harvested, washed with PBS, followed by addition of 20 μ L of MTT to each well, and incubated for 2 h before 200 μ L DMSO was added. The absorbance was measured on an ELISA reader (Multiskan EX, Lab systems) at a wavelength of 570 nm.

4.3.2. ER- α competitive binding assay:

The ER- α activity assay was carried out using Estrogen Receptor Alpha ELISA Kit (ABCAM, Cambridge, MA), according to the manufacturer's instructions. The absorbance for the tested compounds and controls (Tamoxifen) was measured on an ELISA plate reader at 450 nm.

4.3.3. *In vivo* anticancer activity and safety of YMA-005 and YMA-006:

Swiss albino female mice were used in the present experiment of Ehrlich ascites carcinoma (EAC) solid tumor animal model [27]. On the day of induction, EAC cells were collected from the ascitic fluid of a female mouse bearing ascitic tumor, diluted with sterile saline to produce $\sim 12.5 \times 10^6$ per 1 mL. 0.2 mL was then injected intramuscularly in the left thigh of all female mice. When mice developed palpable mass (~ 100 mm³), treatment was started (day 0). EAC-

bearing mice received a once weekly i.p. injection of either, fulvestrant (FULV) at a dose of 5 mg/mouse as well as YMA-005 and YMA-006 at a dose of 5 and 10 mg/mouse for each. Treatments were delivered in 10% Tween 80 starting 5 days after inoculation. Mice in the control groups received drug vehicles. Tumor volume was measured using a digital caliper at different times after treatment, according to the following equation:

$$\text{Tumor volume (mm}^3\text{)} = \text{Length (mm)} \times [\text{Height (mm)}]^2 \times 0.52$$

Mice belonging to different groups were overnight food-deprived before scarification under anesthesia after 15 days of starting treatment. Tumor tissues were then collected for further analysis.

The safety of YMA-005 and YMA-006 was observed in normal mice at a single dose of 10 mg/mouse, i.p., where they were monitored for short-term acute signs of toxicity or mortality for 7 days. All experimental procedures were carried out in accordance with the National Institutes of Health guide for the care and use of Laboratory animals.

Histopathological analysis:

Tumors were collected, fixed in 10% formalin solution, and embedded in paraffin. They were stained with hematoxylin and eosin (H&E) to examine the histopathological changes. Moreover, the necrotic index for each group was determined in 10 random fields per section per animal in the treated and control groups using Leica application computer analyzer system.

4.3.4. Immunohistochemical analysis:

Immunohistochemistry was performed using an avidin-biotin complex immunoperoxidase technique with anti-mouse primary monoclonal antibody against ER- α receptor diluted at 1:100, in PBS. For detection, a streptavidin-biotin-peroxidase preformed complex and peroxidase- 3,3'-

diaminobenzidine (DAB) were used, according to the manufacturer's instructions. Sections were counterstained with Mayer's hematoxylin and mounted with DPX medium. Positive and negative control slides were included. Tumor section with no primary antibody was used as negative control. Percentage of positively stained cells correlated with the expression of ER- α was estimated in 10 random fields per section per animal using Leica application computer analyzer system [28].

4.3.5. Statistical analysis: Data are presented as mean \pm S.D., and analyzed by one-way analysis of variance (One-way ANOVA) followed by Tukey Kramer *post hoc* test for multiple comparisons using GraphPad Prism version 5 (GraphPad Software, CA, USA). Values of $P < 0.05$ were considered to be statistically significant.

5. Acknowledgments:

The British University in Egypt (BUE) funded this research; grant number [YIRG-2016-01]. The authors appreciate the support offered by OpenEye molecular modeling software for sharing an academic license.

6. References:

- [1] American Cancer Society. Breast Cancer Facts and Figures 2017-2018. Atlanta: American Cancer Society, Inc. 2017.
- [2] M.H. Zhang, H.T. Man, X.D. Zhao, N. Dong, S.L. Ma, Estrogen receptor-positive breast cancer molecular signatures and therapeutic potentials, *Biomed. Rep.* 2 (2013) 41-52.
- [3] C. Sotiriou, S. Neo, L. McShane, Breast cancer classification and prognosis based on gene expression profiles from a population-based study, *Proc. Natl. Acad. Sci.* 100 (2003) 10393-10398.

- [4] H. Lee, T. Kim, K. Choi, Functions and physiological roles of two types of estrogen receptors, ER α and ER β , identified by estrogen receptor knockout mouse, *Lab Anim. Res.* 28 (2012) 71-76.
- [5] P. Huang, V. Chandra, F. Rastinejad, Structural overview of the nuclear receptor superfamily: insights into physiology and therapeutics, *Annual Rev. Physiol.* 72 (2010) 247-272.
- [6] P. Egea, B. Klaholz, D. Moras, Ligand–protein interactions in nuclear receptors of hormones. *FEBS Lett.* 476 (2000) 62-67.
- [7] K. Dhingra, Antiestrogens--tamoxifen, SERMs and beyond, *Invest. New Drugs* 17 (1999) 285-311.
- [8] P. Maximov, J. Lewis-Wambi, V. Jordan, The Paradox of Oestradiol-Induced Breast Cancer Cell Growth and Apoptosis, *Curr. Signal Transduct. Ther.* 4 (2009) 88-102.
- [9] W. Fan, J. Chang, P. Fu., Endocrine therapy resistance in breast cancer: Current status, possible mechanisms and overcoming strategies, *Future Med. Chem.* 7 (2015) 1511-1519.
- [10] S. Srinivasan, J. Nwachukwu, N. Bruno, V. Dharmarajan, D. Goswami, I. Kastrati, S. Novick, J. Nowak, V. Cavett, H. Zhou, N. Boonmuen, Y. Zhao, J. Min, J. Frasor, B. Katzenellenbogen, P. Griffin, J. Katzenellenbogen, K. Nettles, Full antagonism of the estrogen receptor without a prototypical ligand side chain, *Nat. Chem. Biol.* 13 (2016) 111-118.
- [11] A. Alsayari, L. Kopel, M.S. Ahmed, A. Pay, T. Carlson, F. Halaweish, Design, synthesis, and biological evaluation of steroidal analogs as estrogenic/anti-estrogenic agents, *Steroids* 118 (2017) 32-40.
- [12] R. Xiong, J. Zhao, L. Gutgesell, Y. Wang, S. Lee, B. Karumudi, H. Zhao, Y. Lu, D. Tonetti, G. Thatcher, Novel Selective Estrogen Receptor Down regulators (SERDs) Developed against Treatment-Resistant Breast Cancer, *J. Med. Chem.* 23 (2017) 1325-1342.
- [13] A. Brzozowski, A. Pike, Z. Dauter, R. Hubbard, T. Bonn, O. Engström, L. Ohman, G. Greene, J. Gustafsson, M., Carlquist, Molecular basis of agonism and antagonism in the oestrogen receptor, *Nature* 389 (1997) 753-758.
- [14] S. Lee S, M. Barron, Structure-Based Understanding of Binding Affinity and Mode of Estrogen Receptor α Agonists and Antagonists, *PLoS One* 12 (2017) e0169607.

- [15] V. Delfosse, A. Maire, P. Balaguer, W. Bourguet, A structural perspective on nuclear receptors as targets of environmental compounds, *Acta Pharmacol. Sin.* 36 (2014) 88-101.
- [16] S. Nelsen, Y. Luo, M. Weaver, J. Lockard, J. Zink, Optical spectra of protected diamine 10-bond-bridged inter valence radical cations related to N, N, N',N'-tetraalkylbenzidine, *J. Org. Chem.* 71 (2006) 4286-4295.
- [17] X. Wang, B. Lane, D. Sames, Direct C-arylation of free (NH)-indoles and pyrroles catalyzed by Ar-Rh(III) complexes assembled in situ, *J. Am. Chem. Soc.* 127 (2005) 4996-4997.
- [18] S. Heller, E. Schultz, R. Sarpong, Chemoselective N-acylation of indoles and oxazolidinones with carbonylazoles, *Angew. Chem. Int. Ed. Engl.* 51 (2012) 8304-8308.
- [19] S. Annedi, S. Maddaford, G. Mladenova, J. Ramnauth, S. Rakhit, J. Andrews, D. Lee, D. Zhang, F. Porreca, D. Bunton, L. Christie, Discovery of N-(3-(1-methyl-1,2,3,6-tetrahydropyridin-4-yl)-1H-indol-6-yl) thiophene-2-carboximidamide as a selective inhibitor of human neuronal nitric oxide synthase (nNOS) for the treatment of pain, *J. Med. Chem.* 54 (2011) 7408-7416.
- [20] S. Musella, V. di Sarno, T. Ciaglia, M. Sala, A. Spensiero, M. Scala, C. Ostacolo, G. Andrei, J. Balzarini, R. Snoeck, E. Novellino, P. Campiglia, A. Bertamino, I. Gomez-Monterrey, Identification of an indole-based derivative as potent and selective varicella zoster virus (VZV) inhibitor, *Eur. J. Med. Chem.* 29 (2016) 773-781.
- [21] M.S. Ahmed, L. Kopel, F. Halaweish, Structural optimization and biological screening of a steroidal scaffold possessing cucurbitacin-like functionalities as B-Raf inhibitors, *ChemMedChem.* 9 (2014) 1361-1367
- [22] P. Hawkins, A. Skillman, G. Warren, B. Ellingson, M. Stahl, Conformer generation with OMEGA: algorithm and validation using high quality structures from the Protein Databank and Cambridge Structural Database, *J. Chem. Inf. Model.* 50 (2010) 572-584
- [23] M.S. Ahmed, F. El-Senduny, J. Taylor, F. Halaweish, Biological screening of cucurbitacin inspired estrone analogs targeting mitogen-activated protein kinase (MAPK) pathway, *Chem. Biol. Drug Des.* 90 (2017) 478-484.
- [24] M. McGann, FRED pose prediction and virtual screening accuracy, *J. Chem. Inf. Model.* 51 (2011) 578-596

[25] OpenEye Toolkits 2017. Oct.1 OpenEye Scientific Software, Santa Fe, NM. <http://www.eyesopen.com>.

[26] T. Mosmann, Rapid colorimetric assay for cellular growth and survival: application to proliferation and cytotoxicity assays, *J. Immunol. Meth.* 65 (1983) 55-63

[27] S.K. Jaganathan, D. Mondhe, Z.A. Wani, H.C. Pal, M. Mandal, Effect of honey and eugenol on Ehrlich ascites and solid carcinoma, *J. Biomed. Biotechnol.* 2010 (2010) 989163.

[28] S.M. Hsu, L. Raine, H. Fanger, Use of avidin-biotin-peroxidase complex (ABC) in immunoperoxidase techniques: a comparison between ABC and unlabeled antibody (PAP) procedures, *J. Histochem. Cytochem.* 29 (1981) 577-580.

List of Figures and Tables:

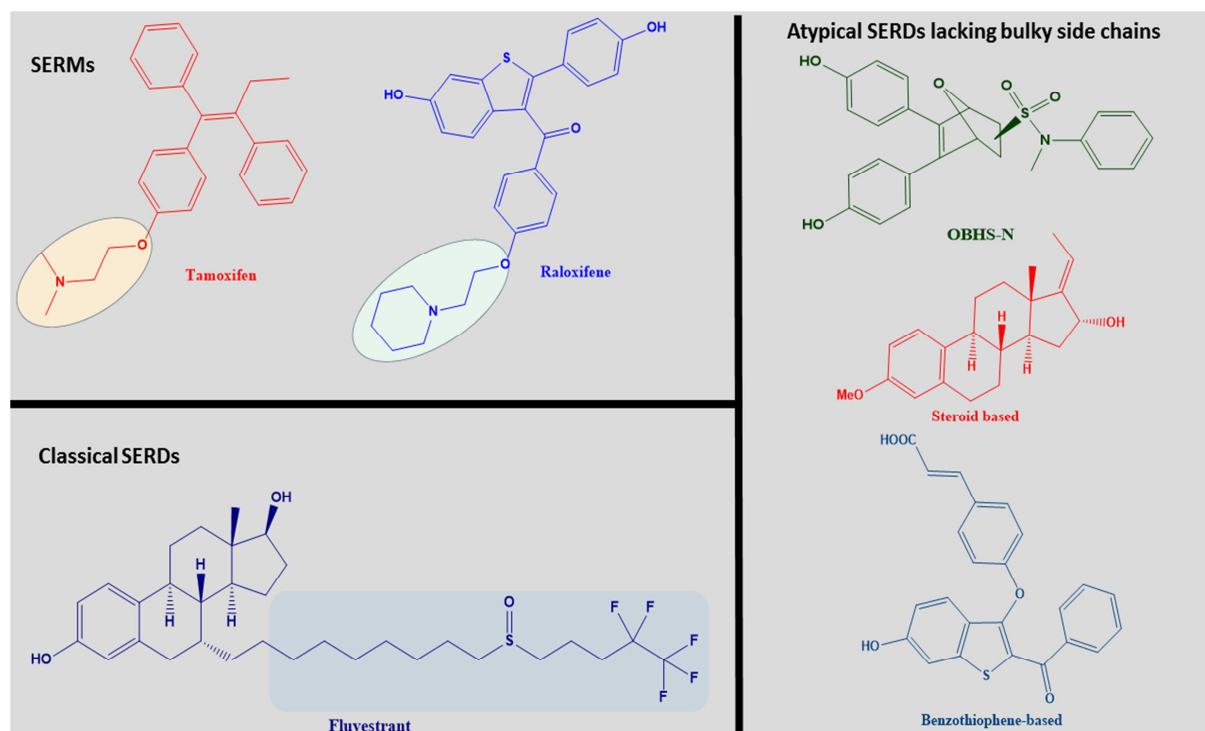


Figure 1. Examples for selective estrogen receptor modulator (SERM), classical selective estrogen receptor down regulator (SERD), and atypical SERD lacking side chain

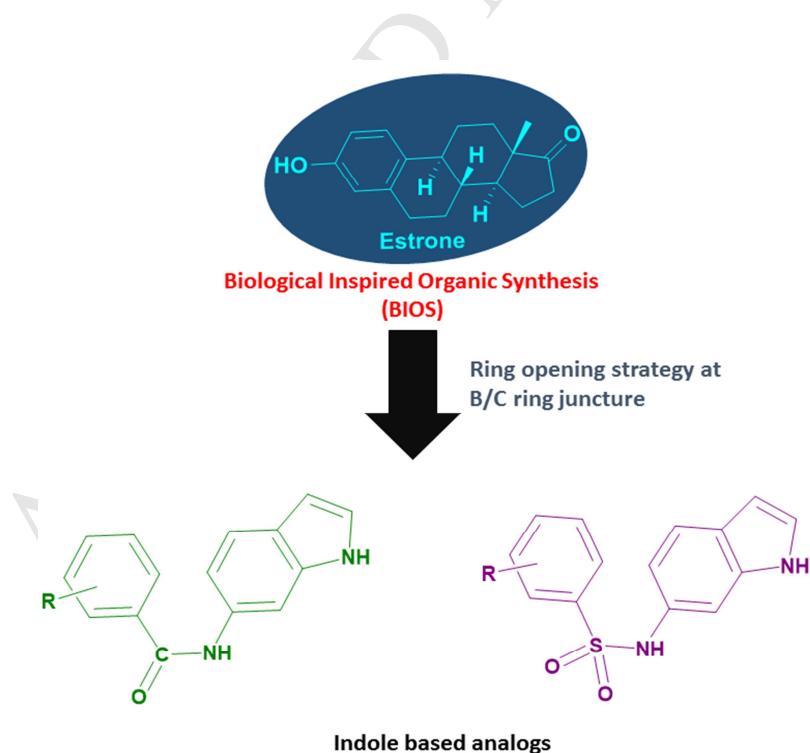
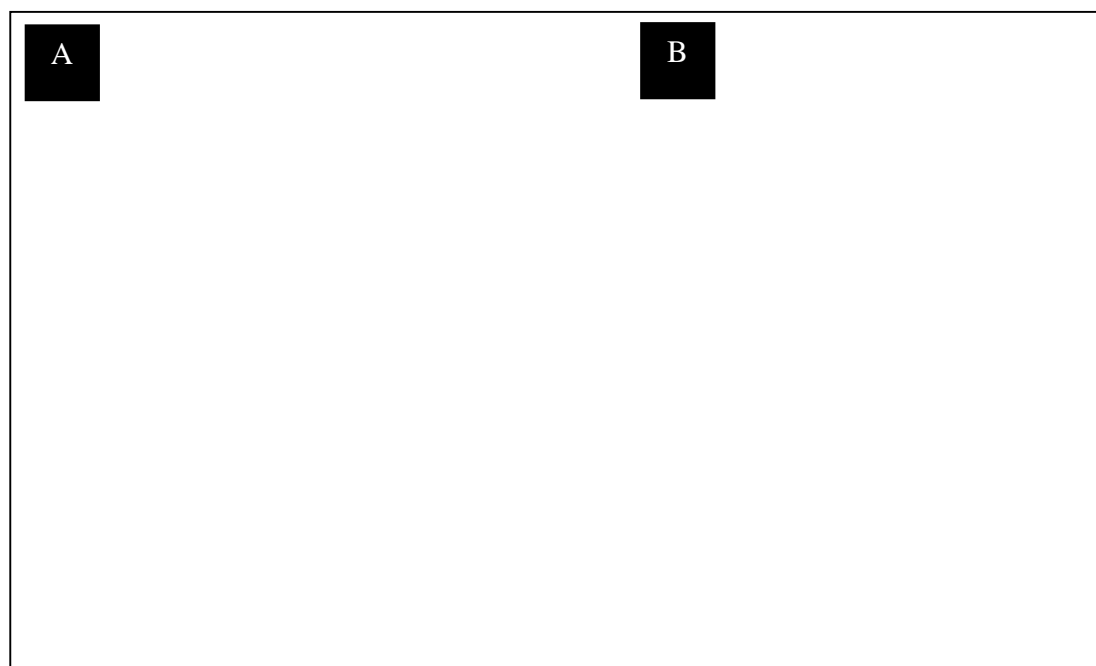
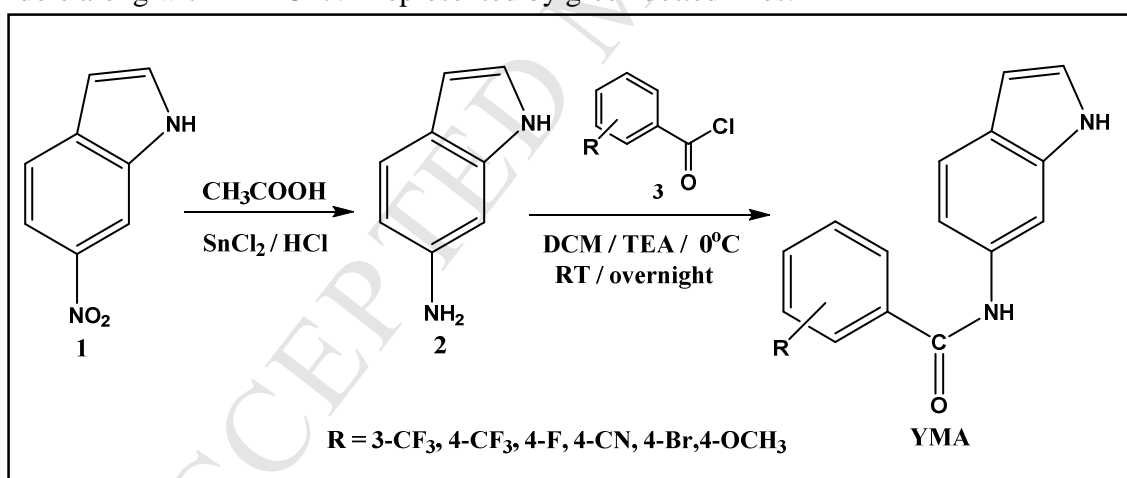


Figure 2. Design strategy to assemble indole-based biomimetic analogs



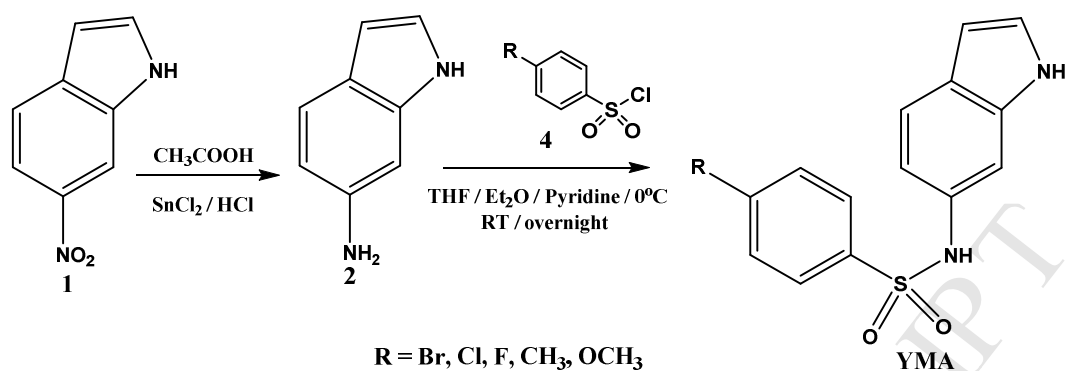
Figure

and (B) Sulfonamide bond along with estrogen receptor alpha (PDB ID: 1ERE), showing the hydrophobic interactions with the ligand binding domain and hydrogen bond interactions of $-NH$ of indole along with THR 347:A represented by green dotted lines.



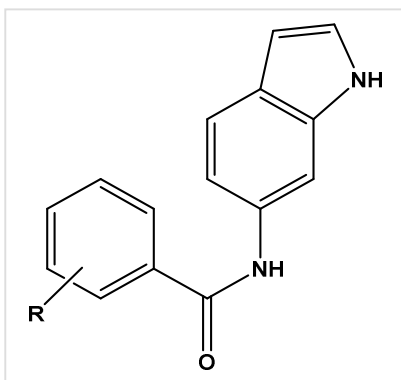
Scheme 1. Assembly of YMA-001 to YMA-005 analogs





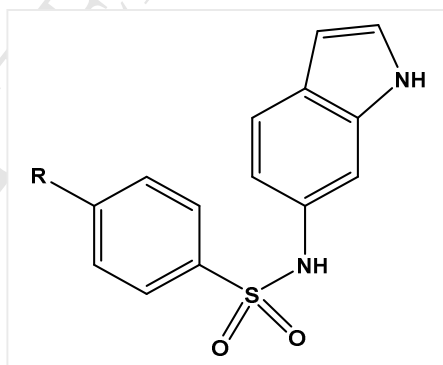
Scheme 2. Assembly of YMA-006 to YMA-010 analogs

Table 1. Inhibitory activity of indole-based analogs against estrogen receptor dependent cancer cell lines and ER- α ELISA competitive binding assays



Compound	R	Molecular weight (g/mol)	IC ₅₀ MCF-7 (μ M)	IC ₅₀ T-47D (μ M)	IC ₅₀ (ER - α) (nM)
----------	---	--------------------------	-----------------------------------	-----------------------------------	--

YMA-001	4-F	254.09	45.93 ± 0.98	35.06 ± 0.75	69.46
YMA-002	4- CF ₃	304.27	63.43 ± 2.14	51.34 ± 0.98	8.15
YMA-003	4-CN	261.28	33.56 ± 0.46	35.75 ± 0.95	2.40
YMA-004	4-Br	315.17	38.14 ± 0.85	63.74 ± 2.30	4.71
YMA-005	3-CF ₃	304.27	30.63 ± 0.72	28.23 ± 0.95	1.76
	Tamoxifen	371.51	42.40 ± 0.78	34.42 ± 0.83	1.50



Compound	R	Molecular weight (g/mol)	IC ₅₀ MCF-7 (μM)	IC ₅₀ T-47D (μM)	IC50 (ER – α) (nM)
YMA-006	F	290.31	30.89 ± 0.96	32.96 ± 0.69	3.31
YMA-007	Cl	306.76	54.02 ± 0.84	46.16 ± 1.76	44.43
YMA-008	CH ₃	286.35	37.2 ± 1.20	57.13 ± 1.43	204.75
YMA-009	Br	351.22	37.75 ± 1.08	40.06 ± 1.53	22.67

YMA-010	OCH ₃	302.35	57.22 ± 2.02	45.04 ± 0.89	7.53
---------	------------------	--------	--------------	--------------	------

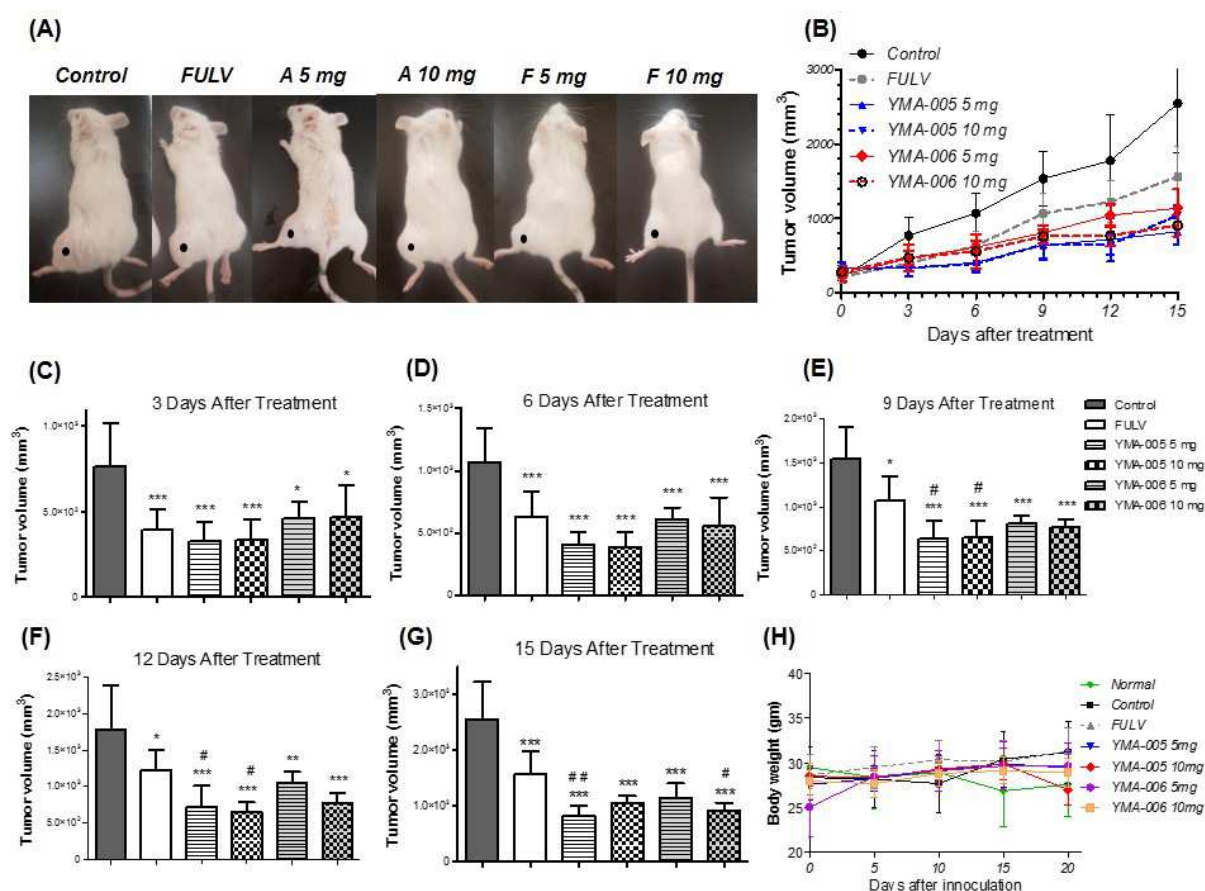


Figure 4. (A) EAC solid tumor-bearing mice in control and YMA-005- and YMA-006-treated groups at 15 days of treatment. (B) Tumor volume (mm³) in EAC-bearing mice of control and treated groups at different time points. (C-G) Bar charts showing tumor volume (mm³) at 3, 6, 9, 12, and 15 days of treatment. (H) Body weight of animals in treated and control groups, at different time points. Values are presented as means ± SD (n=10). One-way analysis of variance (One-way ANOVA) followed by Tukey Kramer post hoc test was applied for statistics. Significant difference compared to control at *P<0.05, **P<0.01, ***P<0.001. Significant difference compared to FULV at #P<0.05, ##P<0.01

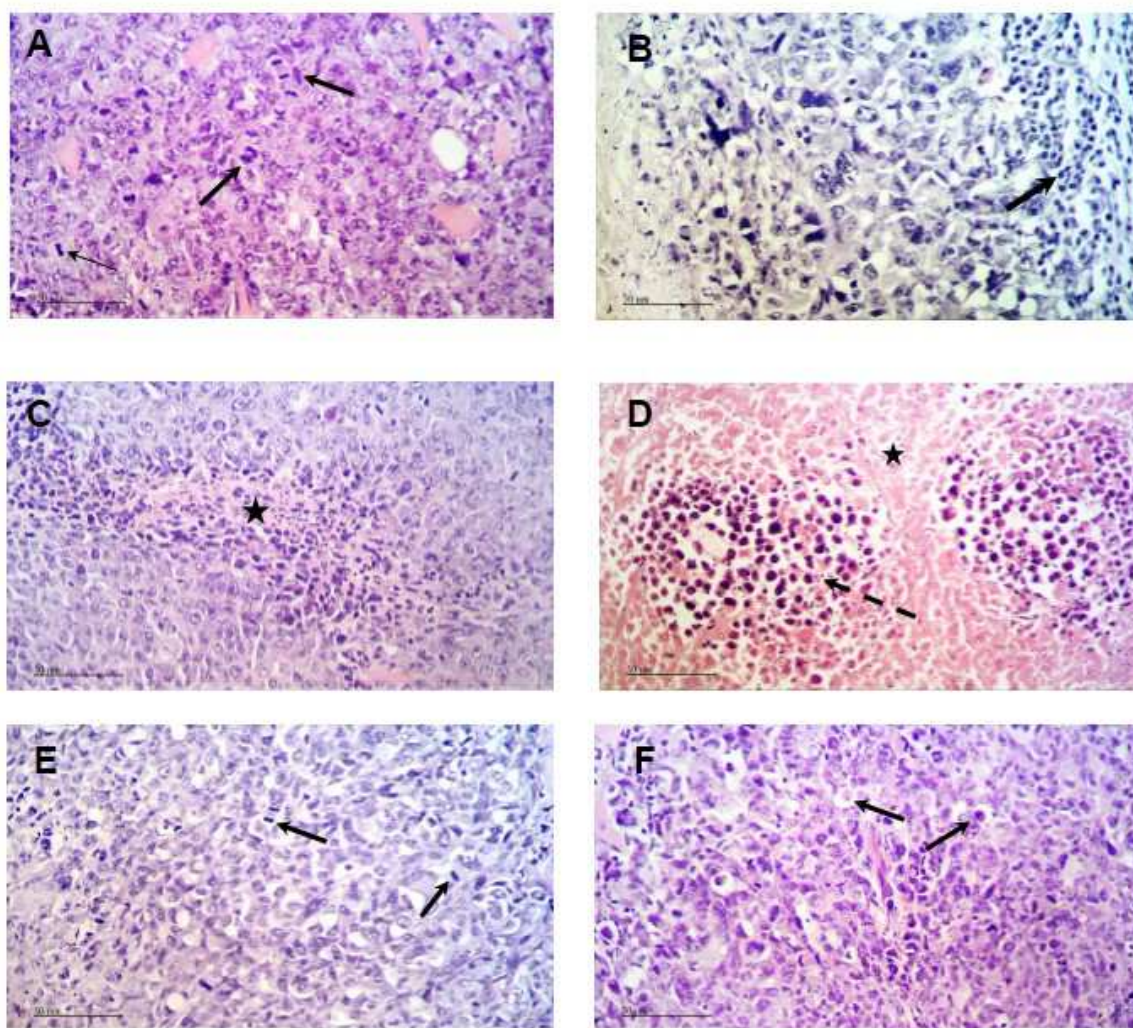


Figure 5. Photomicrographs of H&E-stained tumor sections (X400) in (A) control group showing widespread viable tumor cells sheets with many mitotic figures (arrows) and prominent nucleoli in the outer zone of tumor mass. Limited small area of necrotic tissue was observed in

the deeper zone of the examined sections (star), **(B)** Fulvestrant- and **(C)** YMA-005 (5 mg)-treated groups showing moderate size areas of necrosis and degenerated cells (star), infiltrated by viable sheets of tumor cells as well as inflammatory cells (arrow), **(D)** YMA-005 (10 mg)-treated group demonstrating the most extensive necrotic areas (star) as well as degenerated tumor cells (dashed arrow), **(E)** YMA-006 (5 mg)-treated group showing tumor sections with the least areas of necrosis, and **(F)** YMA-006 (10 mg)-treated group showing mixed viable and focal necrotic areas (star) in deeper parts of tumor mass. Scattered apoptotic cells were observed (arrows) between viable active tumor cells.

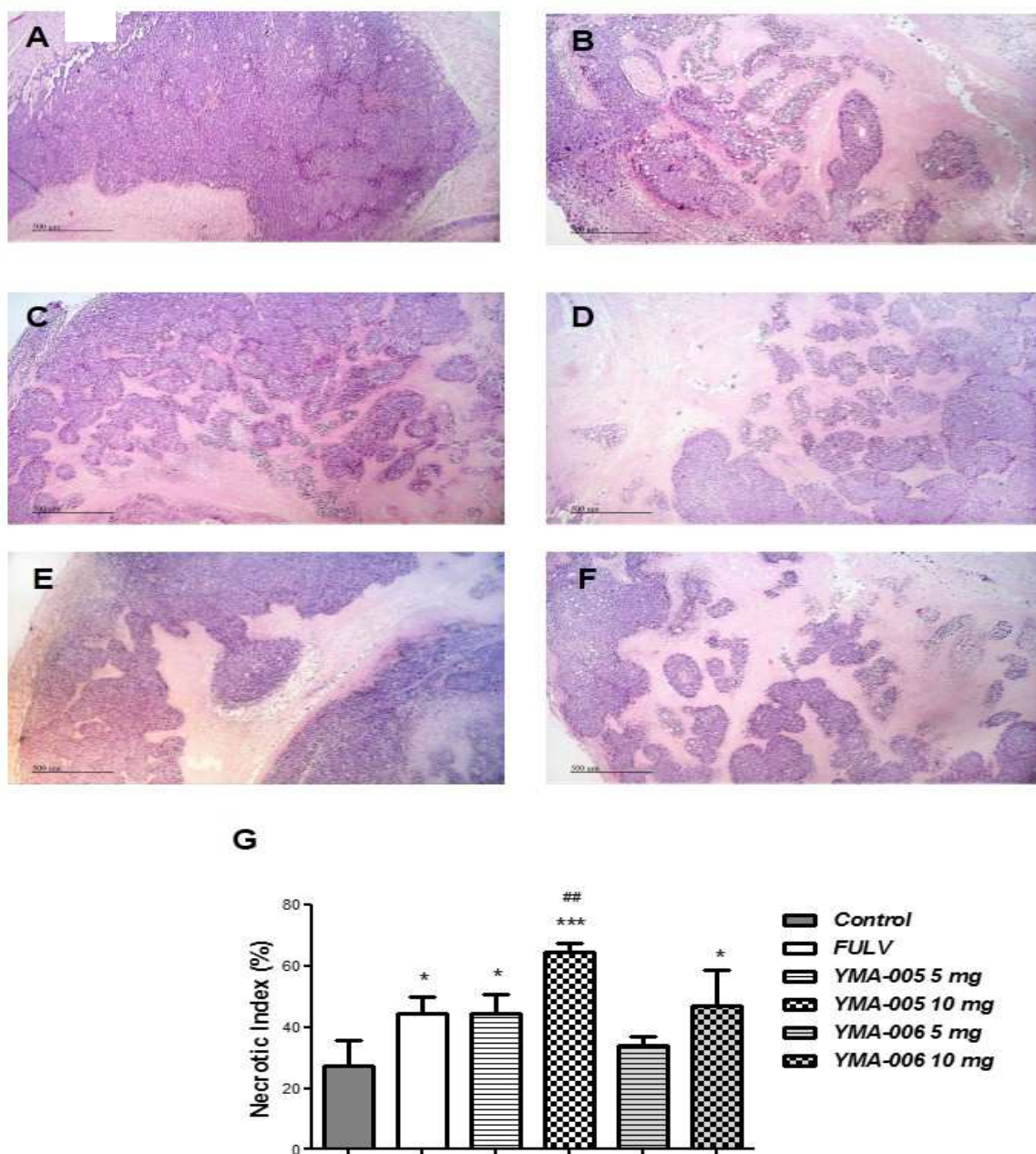


Figure 6. Photomicrographs of H&E-stained tumor sections (X100) showing areas of necrosis in (A) control group and groups treated with (B) fulvestrant, (C) YMA-005 (5 mg), (D) YMA-005 (10 mg), (E) YMA-006 (5 mg), and (F) YMA-006 (10 mg). (G) Necrotic indices as assessed in H&E-stained tumor sections in control and treated groups. Values are presented as means \pm SD (n=10). One-way analysis of variance (One-way ANOVA) followed by Tukey Kramer post hoc test was applied for statistics. Significant difference compared to control at * P <0.05, *** P <0.001. Significant difference compared to FULV at ## P <0.01.

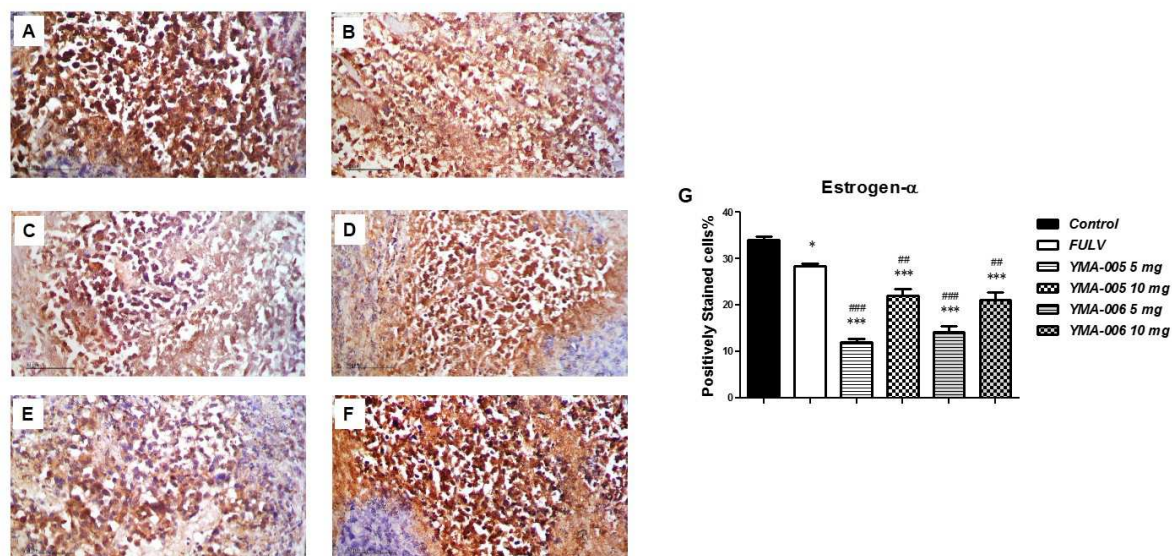


Figure 7. Photomicrographs of immunohistochemically staining (immunostain, DAB, X400) using primary monoclonal antibody against estrogen-alpha (ER- α) receptor in tumor sections from (A) control group and groups treated with (B) fulvestrant, (C) YMA-005 (5 mg), (D) YMA-005 (10 mg), (E) YMA-006 (5 mg), and (F) YMA-006 (10 mg). (G) Immunohistochemical expression of ER- α in tumor sections of control and treated groups. Values are presented as means \pm SD (n=10). One-way analysis of variance (One-way ANOVA) followed by Tukey Kramer post hoc test was applied for statistics. Significant difference compared to control at *P<0.05, ***P<0.001. Significant difference compared to FULV at ###P<0.001.